Hyperinsulinism induced by targeted suppression of beta cell K_{ATP} channels

J. C. Koster*, M. S. Remedi*, T. P. Flagg, J. D. Johnson, K. P. Markova, B. A. Marshall, and C. G. Nichols†

Department of Cell Biology and Physiology, Washington University School of Medicine, 660 South Euclid Avenue, St. Louis, MO 63110

Edited by Ramon Latorre, Center for Scientific Studies, Valdivia, Chile, and approved November 1, 2002 (received for review August 8, 2002)

ATP-sensitive K^+ (K_{ATP}) channels couple cell metabolism to electrical activity. To probe the role of K_{ATP} in glucose-induced insulin secretion, we have generated transgenic mice expressing a dominant-negative, GFP-tagged K_{ATP} channel subunit in which residues 132–134 (Gly-Tyr-Gly) in the selectivity filter were replaced by Ala-Ala-Ala, under control of the insulin promoter. Transgene expression was confirmed by both beta cell-specific green fluorescence and complete suppression of channel activity in those cells (≈70%) that did fluoresce. Transgenic mice developed normally with no increased mortality and displayed normal body weight, blood glucose levels, and islet architecture. However, hyperinsulinism was evident in adult mice as (*i*) a disproportionately high level of circulating serum insulin for a given glucose concentration (≈2-fold increase in blood insulin), (*ii*) enhanced glucose-induced insulin release from isolated islets, and (*iii*) mild yet significant enhancement in glucose tolerance. Enhanced glucose-induced insulin secretion results from both increased glucose sensitivity and increased release at saturating glucose concentration. The results suggest that incomplete suppression of K_{ATP} channel activity can give rise to a maintained *hyper*insulinism.

K^+ current | transgenic | pancreas | Kir6.2

The ATP-sensitive K^+ channel (K_{ATP}) has long been proposed as a critical link in glucose-induced insulin release from pancreatic beta cells (Fig. 1*A*; refs. 1 and 2). According to this paradigm, a high intracellular [ATP]/[ADP] ratio in the fed state inhibits K_{ATP} channels, causing membrane depolarization, leading to Ca^{2+} entry through voltage-dependent Ca^{2+} channels and insulin exocytosis. A rise in circulating insulin, in turn, leads to an increased peripheral glucose uptake and compensatory drop in blood glucose. Conversely, a falling intracellular [ATP]/[ADP] ratio during the fasting state is presumed to relieve inhibition of K_{ATP} channels, resulting in membrane hyperpolarization and cessation of Ca^{2+}-induced insulin release (3).

Direct evidence for this paradigm is provided by the stimulatory and inhibitory effects of the K_{ATP}-specific drugs, sulfonylureas and diazoxide, respectively, on insulin secretion *in vivo* (4) and the generation of transgenic and knockout mouse models with expression of altered or deficient pancreatic K_{ATP} (5–7) that exhibit beta cell dysfunction. Profound neonatal diabetes due to permanent suppression of insulin release is observed in transgenic mice expressing overactive beta cell K_{ATP} channels, dramatically illustrating the ability of K_{ATP} channels to inhibit secretion (8). Conversely, the recent discovery of numerous mutations in pancreatic K_{ATP} channel subunits (both the pore-forming Kir6.2 and SUR1) in human patients with persistent hyperinsulinemic hypoglycemia of infancy (PHHI) (3) establishes a causative link between suppressed K_{ATP} activity, and the corollary metabolic disorder of *hyper*insulinism (3). PHHI-associated K_{ATP} mutations can be classified into two major categories: those that suppress channel activity without altering cell-surface expression, and biosynthetic or trafficking defects that reduce or abolish surface expression. In both cases, reduced K_{ATP} channel activity is expected to result in constitutive depolarization, persistently elevated intracellular Ca^{2+} concentration ($[Ca^{2+}]_i$), and unregulated insulin secretion (3). Most patients present with hyperinsulinemia and hypoglycemia within the first few days or first year of life (9). A few cases can be treated with the K_{ATP} channel opener drug diazoxide, but the majority of cases require surgical removal of almost all of the pancreas (9).

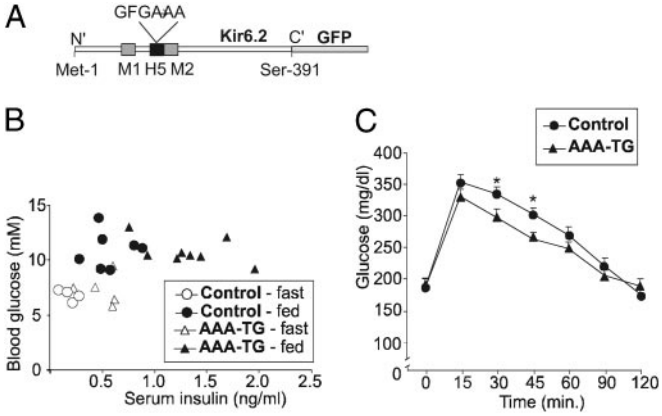

Fig. 1. Hyperinsulinism in AAA-TG mice. (*A*) Schematic of the Kir6.2 subunit. The ion-selectivity pore sequence (^{132}GFG^{134}) in H5 was replaced with –AAA–, and GFP was fused to the C terminus. For transgenic expression, this Kir6.2[AAA]-GFP construct was placed downstream of the rat insulin promoter (RIP-I) driving expression in beta cells. (*B*) Blood sugar vs. insulin levels during both fasting (16 h) and fed states for control and AAA-TG mice aged 4–8 months. Each symbol represents a different animal. (*C*) Glucose-tolerance test results for control and Kir6.2[AAA] male mice age 4–8 months. After administration of glucose load (1.5 g/kg), blood samples from the tail vein were taken at the times indicated and assayed for blood glucose content (*, $P < 0.05$, two-tailed Student's *t* test).

Genetic suppression of Kir6.2 and SUR1 has been undertaken in mice, to probe the roles of K_{ATP} channels *in vivo*. Miki *et al.* (5) generated mice expressing a dominant-negative Kir6.2 mutant (Kir6.2[G132S]) in pancreatic beta cells under insulin promoter control. The G132S mutation perturbs the structure of the K^+-selectivity filter of the channel and renders channels nonfunctional or, perhaps, slightly Na^+-permeable (10). Beta cells from these transgenic mice show reduced K_{ATP} currents, accompanied by a significant increase in both the resting membrane potential and $[Ca^{2+}]_i$ (5). Similar to PHHI phenotypes in humans, they also exhibit hypoglycemia with hyperinsulinemia as neonates. However, these mice develop moderate to severe *hyper*glycemia starting at 4 weeks of age because of extensive loss of beta cell mass through apoptosis. A similar phenotype is observed with both Kir6.2- and SUR1-knockout mice (6, 7), neither of which express any beta cell K_{ATP} channels. Again, these mice show transient hypoglycemia as neonates, but glucose-induced insulin secretion is abolished or highly attenu-

This paper was submitted directly (Track II) to the PNAS office.

Abbreviations: $[Ca^{2+}]_i$, intracellular Ca^{2+} concentration; K_{ATP}, ATP-sensitive K^+ channel; PHHI, persistent hyperinsulinemic hypoglycemia of infancy.

*J.C.K. and M.S.R. contributed equally to this work.

†To whom correspondence should be addressed. E-mail: cnichols@cellbio.wustl.edu.

www.pnas.org/cgi/doi/10.1073/pnas.012479199

ated in adults, and the mice are normoglycemic (6, 7), suggesting a compensatory nonelectrical regulation of secretion.

In the current study, we report the generation of transgenic mice with suppressed pancreatic K_{ATP} currents that demonstrate hyperinsulinism as adults, but not as neonates. Transgenic mice demonstrate significantly higher circulating insulin levels, and enhanced glucose-induced insulin release from isolated islets compared with control littermates, together with increased pancreatic insulin content. These mice provide a unique model of K_{ATP}-dependent hyperinsulinism and lead us to suggest a unifying hypothesis to explain the consequences of suppression of beta cell K_{ATP} channel activity.

Experimental Procedures

Generation of Transgenic AAA-TG Line. The Kir6.2[AAA]-GFP construct (Fig. 1) was generated by replacing the tripeptide ^{132}GFG^{134} of the ion selectivity filter of Kir6.2 with nonpolar alanine residues, and by C-terminally tagging with enhanced GFP (EGFP) (Fig. 1). The generation of the transgenic mouse (AAA-TG) line was described in ref. 8. One Kir6.2[AAA] founder was identified and bred back to C57BL/6 mates to establish a permanent line. F_2–F_7 mice were used in all experiments.

Isolation of Pancreatic Islets and Beta Cells. Anesthetized mice were killed by cervical dislocation. Pancreata were removed and injected with Hank's solution containing collagenase [138 mM NaCl/5.6 mM KCl/4.2 mM $NaHCO_3$/1.3 mM $CaCl_2$/0.44 mM KH_2PO_4/0.4 mM $MgSO_4$/0.3 mM $NaHPO_4$/1 mM EGTA/BSA (1 mg/ml)/5.6 mM D-(+)-glucose/collagenase (1 mg/ml) (pH 7.4)]. Collagenase Type XI was obtained from Sigma. Pancreata were digested for 7 min at 37°C, hand shaken, and washed three times in cold Hank's solution. Islets were hand dissected and pooled. For electrophysiological measurements, islets were washed three times in MEM (MEM without L-glutamine), followed by one wash in DMEM supplemented with trypsin (0.01%) and EDTA (0.002%), and a final wash in DMEM. Trypsin-treated islets were dispersed by resuspending gently in complete RPMI medium 1640 [supplemented with FCS (10%), penicillin (100 units/ml), and streptomycin (100 μg/ml)]. Beta cells were plated on glass coverslips and allowed to attach for 1 h at 37°C and maintained up to 3 days in complete RPMI medium 1640 at 37°C in a humidified incubator.

Immunohistological Analysis. Pancreata were fixed in Streck Tissue Fixative (Streck Laboratories, Omaha, NE) overnight, and paraffin embedded for serial sectioning (5 μm thick). For immunofluorescence, sections were incubated overnight at 37°C with a guinea pig antiinsulin or antiglucagon primary antibodies (1:250 or 1:500, respectively; Linco Research, St. Charles, MO). Primary antibodies were detected by incubating for 1.5 h at 25°C with an anti-guinea pig secondary antibody conjugated with Alexa 488 fluorescent dye (Molecular Probes).

Electrophysiological Measurements. Excised patch-clamp experiments were performed as described (8). The standard bath (intracellular) and pipette (extracellular) solution (K-INT) had the following composition: 140 mM KCl/10 mM K-Hepes/1 mM K-EGTA (pH 7.3). Macroscopic currents in isolated islet cells were recorded using standard whole-cell voltage clamp techniques. Cells were constantly perfused with a bath solution (Tyrode's, containing 137 mM NaCl, 5.4 mM KCl, 1.8 mM $CaCl_2$, 0.5 mM $MgCl_2$, 5 mM Hepes, 3 mM $NaHCO_3$, and 0.16 mM NaH_2PO_4). Electrodes were filled with K-INT plus 1 mM $MgCl_2$ and 1 mM ATP. Two criteria were used to identify beta cells: large cells with capacitance >5 pF and, in the case of transgenic mice, islet cells that fluoresced green. Data were normally filtered at 0.5–3 kHz; signals were digitized at 22 kHz (Neurocorder, Neurodata, New York) and stored on videotape. Experiments were digitized into a microcomputer by using AXOTAPE software (Axon Instruments, Foster City, CA). Off-line analysis was performed using either CLAMPFIT (Axon Instruments) or EXCEL (Microsoft).

Blood Glucose and Insulin Levels. Whole blood was assayed for glucose content using the glucose dehydrogenase-based enzymatic assay and quantitated using the Hemocue glucose meter (Hemocue, Mission Viejo, CA). Insulin levels were assayed in 15 μl of serum using the Rat Insulin RIA kit according to manufacturer's procedure (Linco Research). Intraperitoneal glucose tolerance tests were made on 12- to 20-week-old mice, after 16-h fast. Animals were injected i.p. with glucose (1 g/kg). Blood was isolated from the tail vein at times indicated and assayed for glucose content as described above. Insulin content was assayed in isolated islets of equal diameter ($\approx$100 μm). Islets were sonicated in distilled water, then pelleted for 5 min at 1,000 $\times$ *g*. Supernatant was removed and diluted 1:6,000 for RIA as described above.

Insulin Release Experiments. Pancreatic islets (10 per well) were incubated in glucose-free DMEM supplemented with D-(+)-glucose (1, 7, or 16.7 mM) and either gliblenclamide (1 μM) or diazoxide (250 μM), as indicated. Islets were incubated for 60 min at 37°C and medium removed and assayed for insulin content with Rat Insulin RIA (Linco Research).

Single-Cell $[Ca^{2+}]_i$ Imaging. Islet cell cultures on glass coverslips were incubated at 37°C with 1 μM fura-4F-AM ($Ca^{2+}K_d$ 770 nM; Molecular Probes) in RPMI medium 1640 for 30 min and rinsed in Ringer's solution (5.5 mM KCl/2 mM $CaCl_2$/1 mM $MgCl_2$/20 mM Hepes/144 mM NaCl, and various glucose concentrations isosmotically replacing NaCl) for 30 min. Cells were continuously perfused in a narrow 35°C chamber ($\approx$300 μl) with preheated Ringer's solution. Cells (5–15 per frame) were excited at 340 and 380 nM using a monochromator (TILL Photonics, Planegg, Germany) through a $\times$20 objective (IX70, Olympus, Tokyo) and imaged with a CCD camera (TILL Photonics). Emission ratios (>505 nm) were converted to $[Ca^{2+}]$ after *in vivo* calibration; cells were exposed to 10 μM ionomycin for >30 min to obtain R_{max}, then to 20 μM EGTA/10 μM ionomycin to obtain R_{min}. Ratiometric analysis allows comparison between cells, relatively independently of cell thickness, dye loading, background, and autofluorescence. Under these conditions, interference of enhanced GFP (EGFP) fluorescence is minimal, because the excitation of EGFP is not significant at wavelengths <425 nm, obviating sorting of TG cells into green vs. nongreen cells (see *Results*). Whereas fura-4F fluorescence is largely targeted to the cytosol, cytosolic fluorescence of EGFP-tagged K_{ATP} channels, measured separately under the same conditions, was relatively low (J.D.J., unpublished observations).

Results

Expression of Dominant-Negative Kir6.2[AAA]-GFP Causes Hyperinsulinemia. The Kir6.2[AAA]-GFP founder animal was euglycemic, developed normally, and fertile. Similarly, transgenic (AAA-TG) F_1–F_4 progeny displayed normal body weight and blood sugar levels, both fasting (16 h) and fed, compared with control littermates (Table 1; ref. 8). In neonatal mice (day 4–14), there was also no difference in serum insulin levels between AAA-TG and control littermates (8). However, analysis of serum insulin levels of fasted and fed adult mice (4–8 months) indicated consistently 2.5-fold higher levels in AAA-TG than in control littermates (Table 1, Fig. 1*B*). Adult mice underwent glucose tolerance testing after a 4-h fast. As shown in Fig. 1*C*, AAA-TG mice showed a modest, yet significant increase in glucose excursion and more rapid decline of glucose levels.

Table 1. Phenotypic analysis of adult AAA-TG and littermate control mice

	Control	AAA-TG
Weight, g	25 ± 2	27 ± 2
Blood glucose concentration, mg/dl		
Fasted	119 ± 6	127 ± 12
Fed	197 ± 12	192 ± 8
Serum insulin concentration, pg/ml		
Fasted	200 ± 40	500 ± 80**
Fed	580 ± 80	1300 ± 140**
Free fatty acids, mM (fed)	0.73 ± 0.06	0.77 ± 0.01
Total islets per pancreas	84 ± 5	80 ± 8
Islet diameter, μm	125 ± 4	120 ± 5
Insulin per islet, ng	179 ± 22	311 ± 52*
Resting membrane potential, mV	−65.7 ± 5	−41.4 ± 5.4**
Insulin/blood glucose, pg/ml/mM		
Fasted	30 ± 7	80 ± 10*
Fed	60 ± 10	130 ± 10**
$[Ca^{2+}]_i$, nM (3 mM glucose)	118 ± 10	176 ± 31

Significance: *, $P < 0.05$; **, $P < 0.01$.

AAA-TG Beta Cells Express Variable Levels of Kir6.2[AAA]-GFP. To confirm expression of the Kir6.2[AAA]-GFP protein, islets were isolated from AAA-TG mice at ages 4–8 months (Fig. 2). Beta cell-specific green fluorescence is only present in AAA-TG islets, and all AAA-TG islets fluoresce with similar intensity. However, GFP expression within each islet, assessed by visual estimation of the number of fluorescing beta cells after cell dispersion, or by fluorescent confocal microscopy of whole islets, indicates incomplete penetrance of the Kir6.2[AAA] transgene. Approximately 70% of beta cells express the GFP-tagged transgene at visibly high levels, but ≈30% show no detectable fluorescence (Fig. 2*B*; for a confocal movie, see Movie 1, which is published as supporting information on the PNAS web site, www.pnas.org, or go to http://128.252.206.141). Such mosaic expression is common in the target tissue of transgenic mice (11–13) and is likely a consequence of the chromosomal site of insertion of the transgene.

Transgenic overexpression of nonfunctional Kir6.2 subunits is predicted to reduce channel activity through incorporation of inactive Kir6.2 subunits into tetrameric channels (14). K_{ATP}

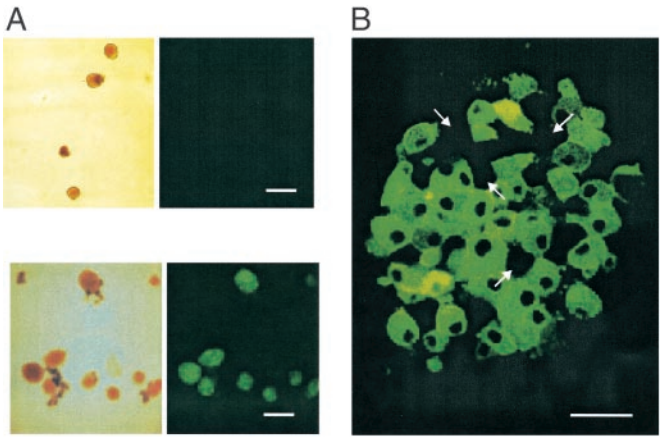

Fig. 2. GFP fluorescence from isolated transgenic islets indicates variegated expression of the Kir6.2[AAA] transgene. (*A*) Clear field and fluorescent images of isolated control (*Upper*) and AAA-TG (*Lower*) islets. (*B*) Representative confocal image (Z section) from a transgenic AAA-TG islet. Arrows denote predicted pancreatic beta cells that do not express the transgene, based on lack of GFP fluorescence. [Scale bars: 100 μm (*A*) and 10 μm (*B*).]

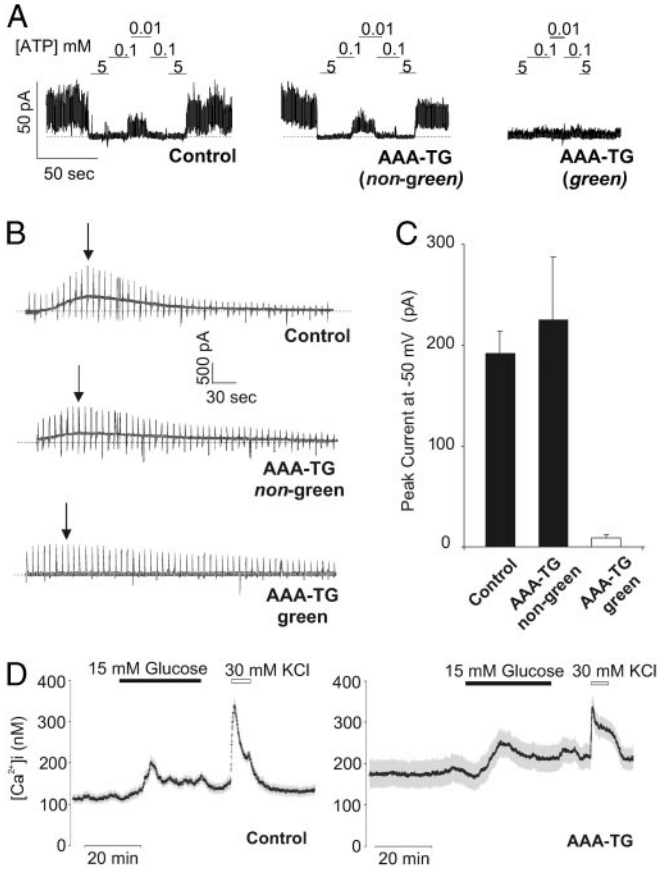

Fig. 3. Green fluorescing AAA-TG beta cells exhibit no detectable K_{ATP} channel activity and elevated $[Ca^{2+}]_i$. (*A*) Representative K_{ATP} currents recorded in inside-out membrane patches from littermate control and AAA-TG beta cells. Patches were exposed to differing ATP concentration as shown. A heterogeneous population of beta cells was observed in the transgenic islets with no K_{ATP} channel activity in the beta cells expressing Kir6.2[AAA]-GFP (green, ≈70%) and the remaining cells (nongreen, ≈30%) displaying wild-type K_{ATP} channels, with respect to channel density and ATP sensitivity. (*B*) Representative macroscopic K^+ current recorded from whole beta cells after dialysis with zero ATP solution (0.5-s ramps from −90 mV to +20 mV delivered every 5 s; holding potential, −50 mV). Peak currents for representative traces are indicated (arrows). (*C*) Averaged peak K^+ currents at −50 mV for AAA-TG (green, $n = 8$; nongreen, $n = 4$) and control beta cells. (*D*) Representative recordings of $[Ca^{2+}]_i$ (symbols; ±SEM) for multiple cells in a field ($n = 28$ and 35, respectively) from a single AAA-TG or control mouse. Cells were exposed to 3 mM glucose or 15 mM glucose, or 30 mM KCl, as indicated. Qualitatively similar results were observed in beta cells from three additional pairs of control and AAA-TG mice.

currents from isolated beta cells were analyzed using inside-out and whole-cell patch clamp techniques. Inside-out membrane patches from green AAA-TG beta cells showed no detectable K_{ATP} channels (Fig. 3*A*). By contrast, patches from nongreen AAA-TG beta cells showed similar channel activity, with similar ATP sensitivity, to patches from control beta cells (Fig. 3*A*). Similarly, large K_{ATP} currents developed after dialysis of control and nongreen AAA-TG beta cells with ATP-free solution, but no K_{ATP} currents developed in green AAA-TG beta cells (Fig. 3 *B* and *C*). The loss of hyperpolarizing K_{ATP} current in green beta cells correlated with a significantly reduced resting potential (Table 1). Consistent with a depolarized membrane potential, Ca^{2+} imaging of dispersed beta cells also reveals elevated mean cytosolic $[Ca^{2+}]_i$ in AAA-TG cells (Table 1, not sorted by green vs. nongreen; see *Experimental Procedures*). The mean response of AAA-TG beta cells to both glucose and KCl-induced rises in

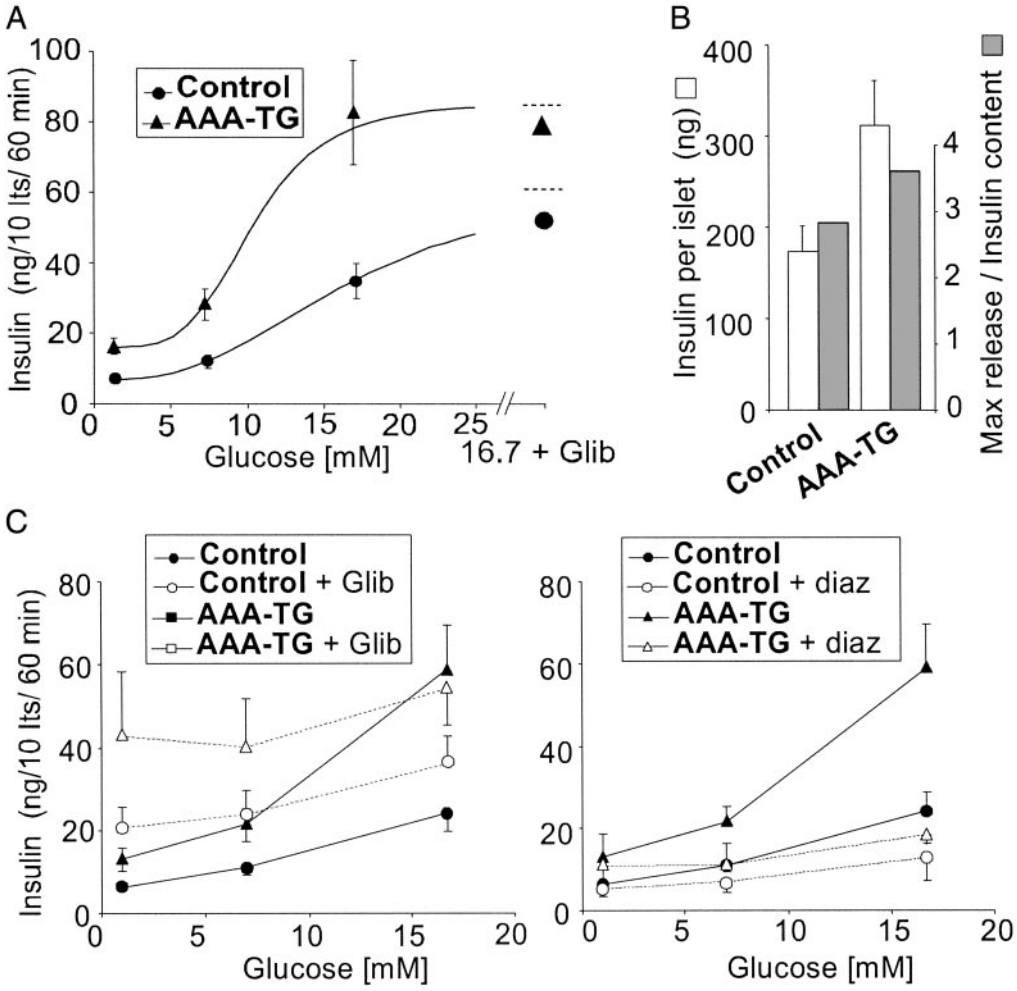

Fig. 4. AAA-TG islets hypersecrete insulin. (*A*) Glucose dependence of insulin secretion from AAA-TG and control islets (n = 17 and 15, respectively) isolated from adult (2–24 months) mice. Also indicated are data obtained in the presence of 16.7 mM glucose plus 1 μM glibenclamide to estimate maximal release (n = 7 and 8). The curves are fits of the Hill equation with an offset, with $K_{1/2}$ (glucose concentration giving half-maximal stimulated release) = 16.7 and 10.3 mM, and Hill coefficient of 2.7 and 4.3 for control and AAA-TG islets, respectively. (*B*) Insulin content per islet for control and AAA-TG mice (open bars; mean ± SEM; n = 34 and 32), and the ratio of maximal release rate (16.7 mM glucose + glibenclamide) to content (filled bars). (*C*) Glucose dependence of insulin secretion from AAA-TG and control islets (n = 3–6) in the presence or absence of 1 μM glibenclamide or 250 μM diazoxide (paired experiments).

$[Ca^{2+}]_i$ are decreased (Fig. 3*D*). Taken together, the electrophysiologic and Ca^{2+}-imaging data are consistent with suppression of K_{ATP} current, depolarization, and elevation of $[Ca^{2+}]_i$ in transgenic beta cells.

Insulin Hypersecretion from AAA-TG Islets. As shown in Fig. 4*A*, isolated islets from adult (2–24 months) AAA-TG mice display elevated insulin release at both nonstimulatory (1 mM) and stimulatory (≥7 mM) glucose concentrations, compared with control mice. Moreover, glucose responsiveness is enhanced (i.e., the dose–response curve is shifted to the left) and the maximal response is elevated. This hypersecretion is likely to account for the significantly elevated serum insulin levels and increased glucose tolerance in transgenic Kir6.2[AAA] mice during both fed and fasting states (Table 1). Beta cell insulin content is also significantly higher in transgenic islets (Fig. 4*B*, Table 1), at least partially accounting for the elevated maximal insulin release.

Sulfonylurea drugs, such as glibenclamide, inhibit K_{ATP} channels and can maximally stimulate insulin secretion. As shown in Fig. 4*C*, glibenclamide elevates insulin release to an almost constant, maximal level in both AAA-TG and control islets, but the maximal level in AAA-TG is almost double that in control. Diazoxide, a K_{ATP} channel opener, suppresses insulin secretion to a minimal level at all glucose concentrations in both AAA-TG and control islets. Again, the minimal level is higher in AAA-TG than in control islets, further consistent with elevated insulin content in AAA-TG islets. The ability of diazoxide to suppress secretion at all glucose levels in AAA-TG islets indicates that, although K_{ATP} channel activity is present in only ≈30% of cells, electrical coupling ensures that this is still sufficient to suppress secretion from the whole islet when activated.

Normal Islet Morphology Is Maintained in Kir6.2[AAA] Islets. Immunohistochemical analyses were performed on sectioned pancreata from mice aged 3–4 months. Immunostaining of insulin-containing beta cells from a AAA-TG pancreas reveals normal islet size and distribution (Fig. 5, Table 1). Redistribution of alpha cells and qualitative loss of beta cell mass (as defined by reduced immunofluorescence), which are characteristic of Kir6.2$^{-/-}$ (6) and, to a greater extent, Kir6.2[G123S] (5) mice, are not observed in AAA-TG islets.

Discussion

K_{ATP} Channel Underactivity Can Cause Marked Hyperinsulinism. A long-standing model for glucose-regulated insulin secretion pro-

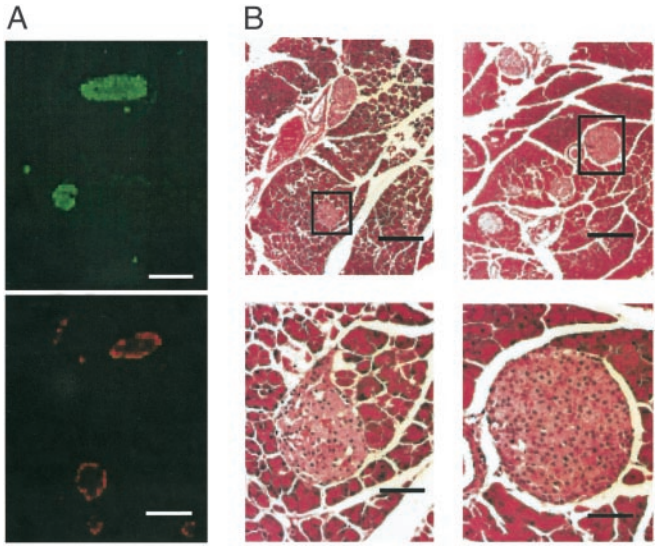

Fig. 5. Hyperinsulinemic AAA-TG islets have normal morphology. (*A*) Representative immunofluorescence of consecutive serial sections of AAA-TG pancreas (5 months) incubated with antiinsulin (*Upper*) or antiglucagon (*Lower*) antibodies. Insulin-containing beta cells form the core of the islet, whereas glucagon-positive alpha cells are found in the periphery, indicating normal islet morphology. (*B*) Representative hematoxylin and eosin staining of pancreatic sections from control (*Left*) and AAA-TG (*Right*) mice. No gross morphological changes were observed in the transgenic islet and the size and distribution of the islets were similar to control sections. Black boxes correspond to regions magnified on right. [Scale bars: 100 μm (*A* and *B Upper*) and 25 μm (*B Lower*).]

poses that beta cell metabolism of glucose leads to elevated cytoplasmic [ATP]/[ADP] ratio, which in turn inhibits K_{ATP} channels, permitting depolarization, Ca^{2+} entry through depolarization-activated Ca^{2+} channels, and fusion of insulin vesicles at the cell surface (15). As discussed above, major support for this model comes from examination of the genetic basis of PHHI. A large percentage of PHHI cases result from recessive mutations in the SUR1 or Kir6.2 genes themselves (9, 16), which cause the "diffuse" form of the disease in which islet appearance is grossly normal. Somatic loss of maternal 11p15 alleles causes "focal" islet hyperplasia due to deletion of growth-inhibitory genes, and unmasks paternal SUR1 or Kir6.2 mutations (9), responsible for the second major group of PHHI. In both cases, the expected consequences of these mutations are either a reduced number of functional K_{ATP} channels, or K_{ATP} channels that are insensitive to a fall in [ATP]/[ADP] ratio and do not open appropriately to suppress insulin secretion (3).

Therefore, a critical test is to demonstrate that beta cell-specific suppression of K_{ATP} channels in an otherwise isogenic background can recapitulate hyperinsulinism. Kir6.2$^{-/-}$ and SUR1$^{-/-}$ mice demonstrate a neonatal hyperinsulinism, although they revert to a hyposecretion and normal blood glucose levels within days (6, 7). Kir6.2$^{-/-}$ and SUR1$^{-/-}$ mice also lack K_{ATP} channels in tissues other than beta cells, which may make it difficult to separate peripheral vs. beta cell-induced effects of K_{ATP} suppression. However, beta cell-specific, dominant-negative Kir6.2[G123S] mice (5) demonstrate neonatal hypoglycemia and again revert to normoglycemia and hyposecretion within a few days. In contrast to these findings, the present AAA-TG mice show normal blood glucose and insulin levels as neonates, but are hyperinsulinemic through adulthood. Two questions arise from these findings: (*i*) What is the mechanistic basis for the hyperinsulinism in these animals? (*ii*) Do the present animals inform the mechanistic basis and progression of human hyperinsulinemia?

Mechanisms Regulating Insulin Secretion. AAA-TG mice demonstrate a very marked suppression of K_{ATP} channel activity; 70% of beta cells express no measurable channel activity, whereas the remaining 30% express apparently normal levels. A leftward shift in the glucose-secretion curve is the primary predicted consequence of the decreased total K_{ATP} conductance. This appears to be one of two distinct contributors to the hyperinsulinism in adult AAA-TG mice, the second being an elevation of peak insulin secretion at saturating glucose concentration, which correlates with, and probably results from, increased insulin content per islet. Although further studies with additional dominant-negative transgenic lines are required, we can speculate that this increase in insulin content is actually a secondary consequence of the left shift in insulin secretory response. At all glucose concentrations, insulin release will be enhanced, and the autocrine action of insulin (17) may then lead to enhanced production and beta cell insulin content.

In the previously characterized K_{ATP}-deficient transgenic and knockout animals, abnormal appearance of peripherally distributed alpha cells among the core of insulin-containing beta cells (5–7) and a decrease in beta cell mass were observed in adult islets (6, 7). This loss of beta cells likely underlies the overt hyperglycemia observed beginning at 4 weeks of age in Kir6.2[G123S] mice. A similar mechanism may cause reversion of hyperinsulinemia to a diabetic phenotype in at least some forms of human PHHI (18). In contrast, immunocytochemistry reveals a normal size and distribution of islets in adult AAA-TG mice. As we consider below, this may reflect a slower progression of the consequence of reduced K_{ATP} activity in AAA-TG than in other animal models, mirroring variable progression of human forms of K_{ATP}-dependent hyperinsulinemia.

Mechanisms of PHHI. PHHI is characterized by dysregulated insulin secretion (19) with a variable clinical phenotype and can be a major cause of severe mental retardation and epilepsy if not treated properly (20–22). Although symptoms of hypoglycemia can appear during the first postnatal hours or days, some cases involving K_{ATP} mutations are only detected months after birth (9). Probably most patients with K_{ATP} defects are diazoxide unresponsive, indicating a significant lack of available channels, and most of these require partial or subtotal pancreatectomy within the first year (9). However, there are patients who carry heterozygous K_{ATP} mutations and have not required surgery. In the extensive case series considered by de Lonlay *et al.* (9), only one of these patients presented with a transient hyperinsulinemia.

The long-term progression of PHHI is complicated in many cases that are treated surgically, but patients generally progress toward diabetes, with unregulated secretion (23) and increased apoptosis (24) that could be a result of increased $[Ca^{2+}]_i$ resulting from maintained depolarization (25, 26). A few PHHI cases have been examined in which there was no surgical treatment. In patients aged 11–13 years old, acute and prolonged insulin secretion were both suppressed, indicating that this progression can occur in untreated cases (18, 27). In each of the previous genetic models of K_{ATP} deficiency [in which beta cell K_{ATP} currents are either completely absent (6, 7) or significantly reduced (5)], neonatal hyperinsulinemia and hypoglycemia very rapidly progressed to hyperglycemia with reduced glucose-induced insulin secretion. Histological analysis revealed abnormal islet architecture, with enhanced apoptosis and a marked decrease in the number of beta cells in adult mice in the dominant-negative and Kir6.2$^{-/-}$ models (5, 6). Adult Kir6.2$^{-/-}$ mice (6) show no glucose-dependent insulin secretion, and older animals are also glucose intolerant. Similarly, in SUR1$^{-/-}$ mice, first-phase insulin release is almost completely abolished and second-phase release is reduced (7). Thus, hyperinsulinism is transient, and frank hypoglycemia with abnormally elevated

insulin/glucose ratios are only observed in the first few days of life. Conceivably, these mice demonstrate a particularly accelerated progression from hyperinsulinemia to diabetes as might occur in the most severe (i.e., completely K_{ATP} channel deficient) versions of human hyperinsulinemia. AAA-TG differ significantly from the knockout mice in that whereas K_{ATP} channels are essentially absent from ≈70% of beta cells, they are present at near-normal density in the remainder. Thus, the phenotype is a partial (i.e., cell-by-cell) knockout. Because of a partial syncitium in the islet (refs. 28 and 29; i.e., cells are electrically coupled to one another), these mice should, and do, still exhibit a K_{ATP} dependence of insulin secretion, but with the set point of electrical activity, and hence secretion, shifted toward lower glucose concentration (Fig. 4*A*). We propose the following hypothesis to explain the different phenotypes resulting from suppression of K_{ATP} channel activity. The initiating consequence of reduced K_{ATP} channel activity (whether due to decreased channel density or failure to activate) will be elevated $[Ca^{2+}]_i$ and insulin hypersecretion, the degree of hypersecretion (and the time of onset) being dependent on the degree of reduction of channel activity. Autocrine stimulation by insulin may further lead to enhanced insulin synthesis and levels within the islet. Conceivably, this reflects the situation in AAA-TG animals, which have a moderate suppression of K_{ATP} activity. Above a threshold level of $[Ca^{2+}]_i$, or other consequent stimulus (17), exhaustion (30–32) and apoptosis (33) gradually leading to beta cell death and decline of insulin secretion may follow. This progression will occur fastest in animals with the lowest levels of K_{ATP} channel activity (i.e., knockout animals).

This hypothesis makes important predictions about human hyperinsulinemia. The most severe (and perhaps most common) forms of the disease, in which K_{ATP} channels are nearly or completely absent, would be expected to progress rapidly to beta cell apoptosis and diabetes, even without intervention. In less severe forms, in which some level of K_{ATP} channel activity remains, this progression may occur more slowly. In the least severe forms of the disease, there may be a slower onset of hyperinsulinemia, and it may be chronically treatable without progression to beta cell failure. Importantly, although a complete lack of K_{ATP} activity has been reported in human PHHI beta cells (34–36), active K_{ATP} channels have been observed in other patient samples (36, 37), consistent with the reduced channel activity that is the result of many disease mutations when they are expressed in recombinant systems (3, 38, 39‡).

‡Cosgrove, K. E., Gonzalez, A. M., Lee, A. T., Barnes, P. J., Hussaim, K., Aynsley-Green, A., Lindley, K. J., Pirotte, B., Lebrun, P. & Dunne, M. J. (2002) *J. Physiol.* **544P,** 21P (abstr.), www.physoc.org/Proceedings/Abstracts/544P/Files/S229.html.

We are very grateful to Dr. Stan Misler for use of his Ca^{2+} imaging facility and for valuable discussions during the course of this work. This work was primarily supported by National Institutes of Health Grant DK55282 (to C.G.N.) and was also supported by the Washington University Diabetes Research and Training Center (Pilot grant support of J.C.K. and reagent support).

1. Cook, D. L., Satin, L. S., Ashford, M. L. & Hales, C. N. (1988) *Diabetes* **37,** 495–498.
2. Misler, S. & Giebisch, G. (1992) *Curr. Opin. Nephrol. Hypertens.* **1,** 21–33.
3. Huopio, H., Shyng, S. L., Otonkoski, T. & Nichols, C. G. (2002) *Am. J. Physiol.* **283,** E207–E216.
4. Gerich, J. E. (1985) *Mayo Clin. Proc.* **60,** 439–443.
5. Miki, T., Tashiro, F., Iwanaga, T., Nagashima, K., Yoshitomi, H., Aihara, H., Nitta, Y., Gonoi, T., Inagaki, N., Miyazaki, J. & Seino, S. (1997) *Proc. Natl. Acad. Sci. USA* **94,** 11969–11973.
6. Miki, T., Nagashima, K., Tashiro, F., Kotake, K., Yoshitomi, H., Tamamoto, A., Gonoi, T., Iwanaga, T., Miyazaki, J. & Seino, S. (1998) *Proc. Natl. Acad. Sci. USA* **95,** 10402–10406.
7. Seghers, V., Nakazaki, M., DeMayo, F., Aguilar-Bryan, L. & Bryan, J. (2000) *J. Biol. Chem.* **275,** 9270–9277.
8. Koster, J. C., Marshall, B. A., Ensor, N., Corbett, J. A. & Nichols, C. G. (2000) *Cell* **100,** 645–654.
9. de Lonlay, P., Fournet, J. C., Touati, G., Groos, M. S., Martin, D., Sevin, C., Delagne, V., Mayaud, C., Chigot, V., Sempoux, C., *et al.* (2002) *Eur. J. Pediatr.* **161,** 37–48.
10. Silverman, S. K., Kofuji, P., Dougherty, D. A., Davidson, N. & Lester, H. A. (1996) *Proc. Natl. Acad. Sci. USA* **93,** 15429–15434.
11. Dobie, K. W., Lee, M., Fantes, J. A., Graham, E., Clark, A. J., Springbett, A., Lathe, R. & McClenaghan, M. (1996) *Proc. Natl. Acad. Sci. USA* **93,** 6659–6664.
12. Engler, P., Haasch, D., Pinkert, C. A., Doglio, L., Glymour, M., Brinster, R. & Storb, U. (1991) *Cell* **65,** 939–947.
13. Allen, N. D., Norris, M. L. & Surani, M. A. (1990) *Cell* **61,** 853–861.
14. Shyng, S. & Nichols, C. G. (1997) *J. Gen. Physiol.* **110,** 655–664.
15. Ashcroft, F. M. & Rorsman, P. (1990) *Biochem. Soc. Trans.* **18,** 109–111.
16. Meissner, T., Beinbrech, B. & Mayatepek, E. (1999) *Hum. Mutat.* **13,** 351–361.
17. Rutter, G. A. (1999) *Curr. Biol.* **9,** R443–R445.
18. Huopio, H., Reimann, F., Ashfield, R., Komulainen, J., Lenko, H. L., Rahier, J., Vauhkonen, I., Kere, J., Laakso, M., Ashcroft, F. & Otonkoski, T. (2000) *J. Clin. Invest.* **106,** 897–906.
19. Aynsley-Green, A., Polak, J. M., Bloom, S. R., Gough, M. H., Keeling, J., Ashcroft, S. J., Turner, R. C. & Baum, J. D. (1981) *Arch. Dis. Child.* **56,** 496–508.
20. Aynsley-Green, A. (1982) *Clin. Endocrinol. Metab.* **11,** 159–194.
21. Meissner, T., Brune, W. & Mayatepek, E. (1997) *Eur. J. Pediatr.* **156,** 754–757.
22. Menni, F., de Lonlay, P., Sevin, C., Touati, G., Peigne, C., Barbier, V., Nihoul-Fekete, C., Saudubray, J. M. & Robert, J. J. (2001) *Pediatrics* **107,** 476–479.
23. Leibowitz, G., Glaser, B., Higazi, A. A., Salameh, M., Cerasi, E. & Landau, H. (1995) *J. Clin. Endocrinol. Metab.* **80,** 386–392.
24. Kassem, S. A., Ariel, I., Thornton, P. S., Scheimberg, I. & Glaser, B. (2000) *Diabetes* **49,** 1325–1333.
25. Chandra, J., Zhivotovsky, B., Zaitsev, S., Juntti-Berggren, L., Berggren, P. O. & Orrenius, S. (2001) *Diabetes* **50,** Suppl. 1, S44–S47.
26. Efanova, I. B., Zaitsev, S. V., Zhivotovsky, B., Kohler, M., Efendic, S., Orrenius, S. & Berggren, P. O. (1998) *J. Biol. Chem.* **273,** 33501–33507.
27. Grimberg, A., Ferry, R. J., Jr., Kelly, A., Koo-McCoy, S., Polonsky, K., Glaser, B., Permutt, M. A., Aguilar-Bryan, L., Stafford, D., Thornton, P. S., *et al.* (2001) *Diabetes* **50,** 322–328.
28. Eddlestone, G. T., Goncalves, A., Bangham, J. A. & Rojas, E. (1984) *J. Membr. Biol.* **77,** 1–14.
29. Sherman, A., Rinzel, J. & Keizer, J. (1988) *Biophys. J.* **54,** 411–425.
30. Kawaki, J., Nagashima, K., Tanaka, J., Miki, T., Miyazaki, M., Gonoi, T., Mitsuhashi, N., Nakajima, N., Iwanaga, T., Yano, H. & Seino, S. (1999) *Diabetes* **48,** 2001–2006.
31. Weir, G. C., Laybutt, D. R., Kaneto, H., Bonner-Weir, S. & Sharma, A. (2001) *Diabetes* **50,** Suppl. 1, S154–S159.
32. Rustenbeck, I. (2002) *Biochem. Pharmacol.* **63,** 1921–1935.
33. Shafrir, E., Ziv, E. & Mosthaf, L. (1999) *Ann. N.Y. Acad. Sci.* **892,** 223–246.
34. MacFarlane, W. M., Chapman, J. C., Shepherd, R. M., Hashmi, M. N., Kamimura, N., Cosgrove, K. E., O'Brien, R. E., Barnes, P. D., Hart, A. W., Docherty, H. M., *et al.* (1999) *J. Biol. Chem.* **274,** 34059–34066.
35. Kane, C., Shepherd, R. M., Squires, P. E., Johnson, P. R., James, R. F., Milla, P. J., Aynsley-Green, A., Lindley, K. J. & Dunne, M. J. (1996) *Nat. Med.* **2,** 1344–1347.
36. Otonkoski, T., Ammala, C., Huopio, H., Cote, G. J., Chapman, J., Cosgrove, K., Ashfield, R., Huang, E., Komulainen, J., Ashcroft, F. M., *et al.* (1999) *Diabetes* **48,** 408–415.
37. Straub, S. G., Cosgrove, K. E., Ammala, C., Shepherd, R. M., O'Brien, R. E., Barnes, P. D., Kuchinski, N., Chapman, J. C., Schaeppi, M., Glaser, B., *et al.* (2001) *Diabetes* **50,** 329–339.
38. Nichols, C. G., Shyng, S. L., Nestorowicz, A., Glaser, B., Clement, J. P., Gonzalez, G., Aguilarbryan, L., Permutt, M. A. & Bryan, J. (1996) *Science* **272,** 1785–1787.
39. Shyng, S. L., Ferrigni, T., Shepard, J. B., Nestorowicz, A., Glaser, B., Permutt, M. A. & Nichols, C. G. (1998) *Diabetes* **47,** 1145–1151.